MONTE CARLO CALCULATIONS OF HIGH-ENERGY NUCLEON-MESON CASCADES AND APPLICATIONS TO GALACTIC COSMIC-RAY TRANSPORT[1]

T. W. Armstrong
R. G. Alsmiller, Jr.
K. C. Chandler

Oak Ridge National Laboratory
Oak Ridge, Tennessee, 37830

Results obtained using a recently developed calculational method for determining the nucleon-meson cascade induced in thick materials by high-energy nucleons and charged pions are presented. The calculational method uses the intranuclear-cascade-evaporation model to treat nonelastic collisions by particles with energies ≳ 3 GeV and an extrapolation model at higher energies. The following configurations are considered: (a) 19.2-GeV/c protons incident on iron, (b) 30.3-GeV/c protons incident on iron, (c) solar and galactic protons incident on the moon, and (d) galactic protons incident on tissue. For the first three configurations, experimental results are available and comparisons between the experimental and calculated results are given.

INTRODUCTION

Nucleon-meson transport calculations that utilize Monte Carlo techniques in conjunction with the intranuclear-cascade-evaporation model for treating nonelastic collisions were previously carried out for a variety of problems involving solar protons and other sources (refs. 1 to 3, for example). The calculational method employed for these problems is restricted to particle energies ≳ 3 GeV because of limitations imposed by the particular intranuclear-cascade model used (ref. 4). To enable transport calculations to be performed for galactic protons and other high-energy sources, the calculational method has been extended to higher energies by using an extrapolation model (ref. 5) to obtain the description of products from nonelastic collisions ≳ 3 GeV. This extrapolation method uses the differential cross sections for the production of nucleons and pions from 3-GeV nucleon-nucleus and 2.5-GeV pion-nucleus collisions as predicted by the intranuclear-cascade-evaporation model, together with energy, angle, and multiplicity scaling relations that are consistent with the sparse experimental data available for high-energy interactions, to estimate the particle production at the higher energies.

[1]This work was partially funded by the National Aeronautics and Space Administration, Order H-38280A, under Union Carbide Corporation's contract with the U. S. Atomic Energy Commission.

This recently developed high-energy transport method has been applied to compute the nucleon-meson cascade induced in thick targets for several source-geometry configurations, and the purpose of the present paper is to present some of the results obtained. The following cases are considered: (a) 19.2-GeV/c protons incident on a thick iron target, (b) 30.3-GeV/c protons incident on a thick iron target, (c) galactic and solar protons incident on the moon, and (d) galactic protons incident on tissue. For the first three cases, experimental data exist so that comparisons with the calculated results can be made in order to check the validity of the calculational method.

RESULTS

19.2-GeV/c Protons Incident on Iron

Citron et al. (ref. 6) have measured the longitudinal and lateral development of the nucleon-meson cascade induced in a thick iron target by a narrow beam of 19.2-GeV/c protons. Figure 1 shows a comparison of the experimental results, the results from the present calculations, and the results available from calculations made by others for the longitudinal development of the cascade. The cascade development is given in terms of both the star density and track intensity. For the present calculations, the star density was calculated using the cross sections for nuclear star production in emulsion given by Hess et al. (ref. 10), and the track intensity was taken to be the flux due to protons above 500 MeV and charged pions above 80 MeV.

In the experiment, the iron absorber consisted of slabs of iron of various thicknesses with air gaps between the slabs. Results for the present calculations in figure 1 are given with and without these air gaps taken into account. As indicated in figure 1, the results of the present calculations for the longitudinal development of the cascade agree reasonably well with the experimental results and with the results from other calculations.

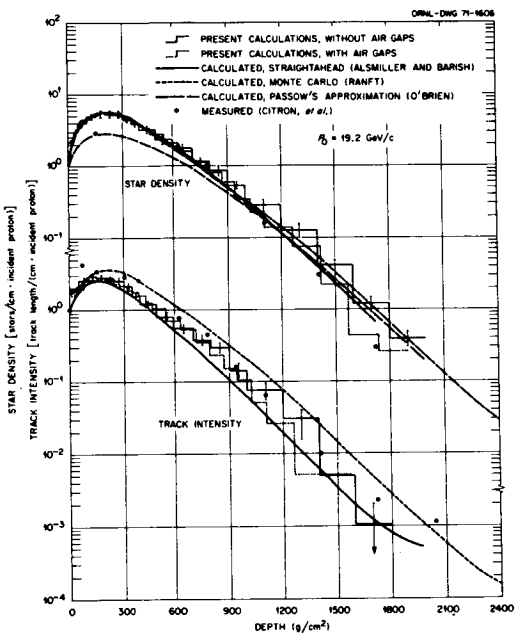

FIGURE 1.— Star density and track intensity versus depth for 19.2-GeV/c protons incident on iron. Results from the present calculations are compared with the straightahead calculations of Alsmiller and Barish (ref. 7), the Monte Carlo calculations of Ranft (ref. 8), the calculations of O'Brien using Passow's approximation (ref. 9), and the measurements of Citron et al. (ref. 6).

The lateral distribution of the track intensity at various depths has also been calculated and compared with the measurements of Citron et al. The calculated and experimental results for the lateral distributions are not in good agreement. The reason for this discrepancy is not known at present. However, as discussed later, the calculated lateral development of the cascade is in good agreement with other experimental data (ref. 11) for 30.3-GeV/c protons incident on iron. In principle, there is no reason that the calculational method should be less accurate for 19.2-GeV/c incident protons than for 30.3-GeV/c incident protons.

30.3-GeV/c Protons Incident on Iron

The lateral development of the nucleon-meson cascade induced in a thick iron target by a narrow beam of 30.3-GeV/c protons has been determined experimentally by Awschalom et al. (ref. 11). The quantity measured was the ^{18}F production in aluminum foils placed at various depths in the iron. Calculations have been carried out to determine the energy and spatial distributions of the nucleon and charged-pion fluxes for this configuration. These fluxes and available cross sections for producing ^{18}F from aluminum (ref. 1) were then used to compute the ^{18}F production as a function of distance from the beam axis. The energy dependence of these cross sections is such that, roughly speaking, the ^{18}F production can be interpreted as a measure of the nucleon and charged-pion fluxes above $\sim$ 50 MeV.

A comparison of the calculated and experimental results is shown in figure 2 for several intermediate depths in the iron. The agreement is quite good although the calculations give a consistently higher production near the beam axis. However, because of the small area and alignment of the aluminum foils used in the experiment, the experimental ^{18}F production is expected to yield an underestimate of the actual production very near

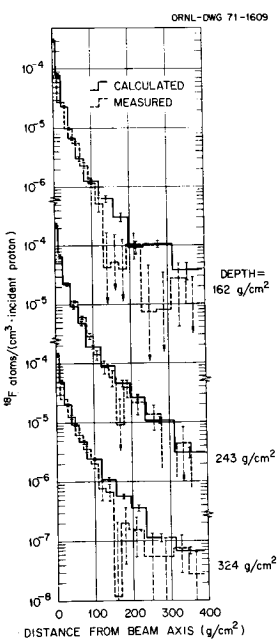

FIGURE 2.— Calculated and measured (ref. 11) lateral distribution of ^{18}F production in aluminum foils at various depths in iron for 30.3-GeV/c incident protons.

the beam axis (ref. 12). The agreement at the intermediate depths shown in figure 2 is fairly typical of the agreement obtained for other comparisons that have been made at depths ranging from 0 to 1045 g/cm^2. The laterally integrated ^{18}F production is not available from the experiment, so the calculated longitudinal development of the cascade cannot be compared with experiment for this case.

Galactic and Solar Protons Incident on the Moon

The depth-dependent radionuclide activity induced in the moon by galactic and solar proton bombardment has been calculated and compared with measurements made on Apollo 11 and 12 samples. As an example of the calculated results obtained, figure 3 shows the depth dependence of the ^{26}Al activity. The total ^{26}Al activity (i.e., the sum of the solar and galactic contributions) is shown in figure 4, together with the measured activity in two moon rocks. Additional comparisons between calculated and measured activities are given elsewhere (ref. 15).

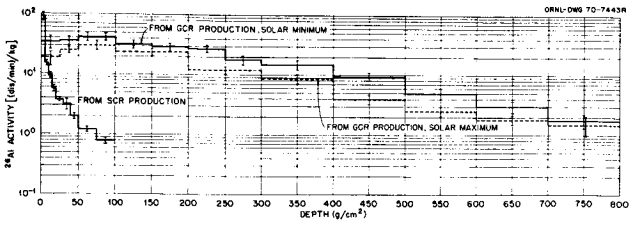

FIGURE 3.— ^{26}Al activity versus depth in moon due to solar cosmic rays (SCR) and galactic cosmic rays (GCR) at solar minimum and solar maximum.

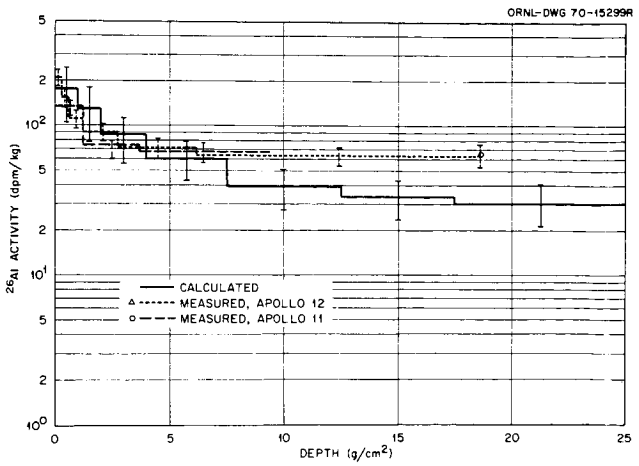

FIGURE 4.— Comparison of calculated and measured (refs. 13, 14) ^{26}Al activity induced in the moon by cosmic-ray bombardment.

The depth dependence of the neutron spectra in the moon has also been calculated. The thermal-neutron flux in the moon has been inferred from the Apollo measurements (ref. 16) and is in good agreement with the calculated flux.

The same calculational method as used here to determine the induced activity in the moon has been applied recently by Gabriel and Santoro to determine the induced activity in the soil surrounding a 500-GeV proton accelerator (ref. 17).

Galactic Protons Incident on Tissue

The absorbed dose and dose equivalent induced by galactic protons in an infinite slab of tissue 30 cm thick have been calculated using the high-energy transport code. An isotropic flux of galactic protons having a solar minimum energy spectrum (ref. 15) was taken to be incident on one side of the tissue slab. The nucleon-meson cascade in the tissue produced by incident protons in the energy range from 30 MeV to 200 GeV was calculated, and the depth dependence of the absorbed dose and dose equivalent was determined as described in reference 18. The electron-photon cascade resulting from the decay of neutral pions and the electrons and positrons from muon decay were taken into account in an approximate manner (ref. 18). The following composition (in at. %) was used for the tissue: H, 63.3; O, 25.8; C, 9.5; N, 1.4. A tissue density of

1.0 g/cm^3 was used.

The absorbed dose and average quality factor as a function of depth in the tissue are shown in figure 5. The average quality factor was computed by dividing the dose equivalent in a given depth interval by the absorbed dose in that interval. In determining the dose equivalent, the quality factors for each type of particle as a function of linear energy transfer were obtained in the same manner as described in reference 17. From figure 5, the absorbed dose for an omnidirectional (over 2π solid angle) flux incident on one side of the tissue slab is approximately 4 rad/y at all depths. For a 4π incident flux (i.e., 2π incident flux on both sides of the slab), the dose would be 8 rad/y, which is in agreement with the value of 10 rad/y quoted by others (refs. 19 and 20) for a 4π flux at solar minimum.

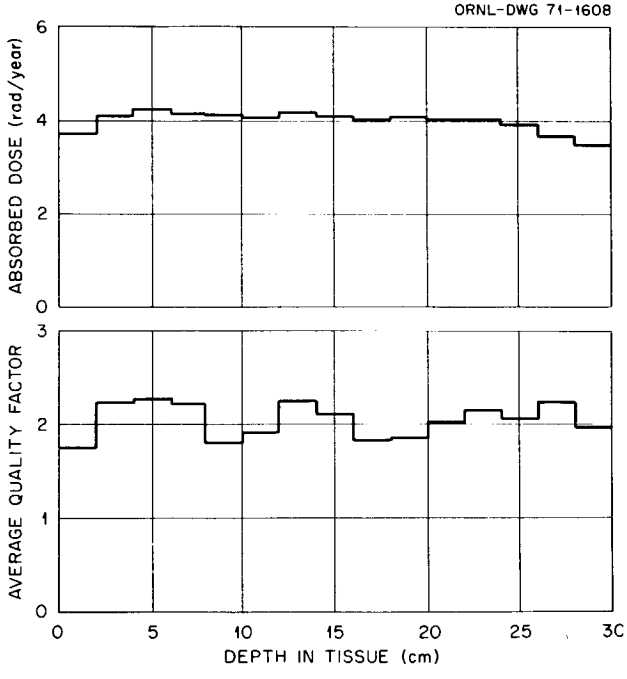

FIGURE 5.— Absorbed dose and average quality factor in tissue from galactic proton bombardment.

The contributions to the absorbed dose and dose equivalent, respectively, from various kinds of particles are shown in figures 6 and 7. The total dose is obtained by adding all of the contributions shown in the figures. The histogram labeled "primary ionization" in figure 6 gives the absorbed dose from the excitation and ionization of atomic electrons by those incident protons which have not undergone nuclear collision. The histogram labeled "secondary protons" gives the absorbed dose from the excitation and ionization of atomic electrons by protons produced from nonelastic nucleon-nucleus and pion-nucleus collisions and from the elastic collisions of nucleons and pions with hydrogen nuclei. The histogram labeled "heavy nuclei" gives the absorbed dose from particles with mass number greater than one produced from nonelastic nucleon-nucleus and pion-nucleus collisions and the absorbed dose from the recoiling nuclei produced from elastic neutron-nucleus collisions and from nonelastic nucleon-nucleus and pion-nucleus collisions. The histogram labeled "charged pions" gives the absorbed dose from the excitation and ionization of atomic electrons by both positively and negatively charged pions produced from nucleon-nucleus and pion-nucleus nonelastic collisions. The histogram labeled "photons from neutral pions" gives the absorbed dose from the electron-photon cascade produced by the photons which arise from the decay of neutral pions. The histogram labeled "electrons, positrons, and photons" gives the

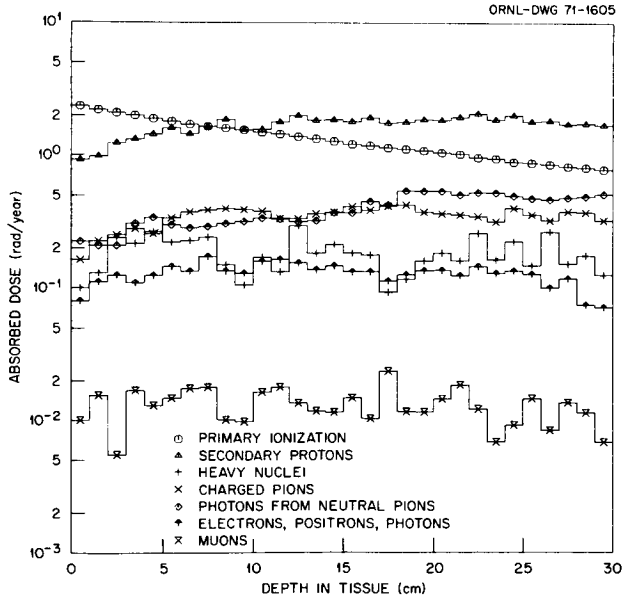

FIGURE 6.— Contribution by particle type to the absorbed dose in tissue from galactic proton bombardment.

absorbed dose from the electrons and positrons produced by muon decay and the absorbed dose from the photons produced by nucleon-nucleus and pion-nucleus nonelastic collisions. The histogram labeled "muons" gives the absorbed dose from the excitation and ionization of atomic electrons by both positively and negatively charged muons. In figure 7 the histograms have similar meanings but give the dose equivalent from these various kinds of secondary particles.

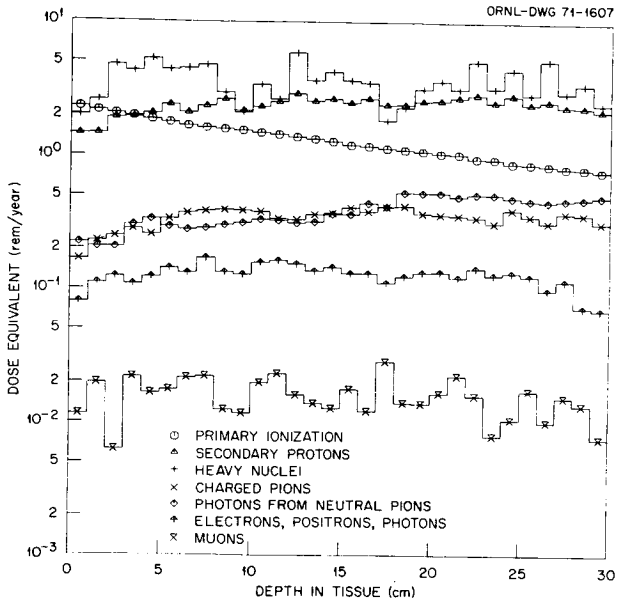

FIGURE 7.— Contribution by particle type to the dose equivalent in tissue from galactic proton bombardment.

It should be realized that only the protons in the cosmic radiation have been considered in calculating the dose. Cosmic-ray nuclei heavier than protons can contribute significantly to the dose, especially at small depths. At present, the transport code used for these calculations is not capable of transporting particles heavier than nucleons.

ACKNOWLEDGMENT

We are very grateful to M. Awschalom, T. Borak, and A. VanGinnekin of the National Accelerator Laboratory for making their preliminary data available to us prior to publication.

REFERENCES

1. ARMSTRONG, T.W.; and ALSMILLER, R.G., Jr.: Nucl. Sci. Eng., Vol. 33, 1968, p. 291.
2. ARMSTRONG, T.W.; and ALSMILLER, R.G., Jr.: Nucl. Sci. Eng., Vol. 37, 1969, p. 337.
3. ARMSTRONG, T.W.; and CHANDLER, K.C.: Calculation of the Radionuclide Production in Tissue by Solar-Flare Bombardment. Neutron Phys. Div. Ann. Progr. Rept. May 31, 1970, Oak Ridge National Laboratory Document ORNL-4592, p.89.
4. BERTINI, Hugo W.: Phys. Rev., Vol. 188, 1969, p. 1711.
5. GABRIEL, T.A.; ALSMILLER, R.G., Jr.; and GUTHRIE, M.P.: An Extrapolation Method for Predicting Nucleon and Pion Differential Production Cross Sections for High-Energy (> 3 GeV) Nucleon-Nucleus Collisions. Oak Ridge National Laboratory Document ORNL-4542, 1970.
6. CITRON, A.; HOFFMAN, L.; PASSOW, C.; NELSON,W.R.; and WHITEHEAD, M.: Nucl. Instr. Meth., Vol. 32, 1965, p. 48.
7. ALSMILLER, R.G., Jr.; and BARISH, J.: Nucl. Instr. Meth., Vol. 36, 1965, p. 309.
8. RANFT, J.: Nucl. Instr. Meth. Vol. 48, 1967, p. 261.
9. O'BRIEN, K.: Nucl. Instr. Meth., Vol. 72, 1969, p. 93.
10. HESS, Wilmot N.; PATTERSON, H. Wade; and WALLACE, Roger: Phys. Rev., Vol. 116, No. 2, 1959, p. 445.
11. Preliminary data of M. Awschalom, T. Borak, and A. VanGinnekin of the National Accelerator Laboratory, to be presented at the International Congress on Protection Against Accelerator and Space Radiation, Geneva, April 26-30, 1971.
12. Van GINNEKIN, A., National Accelerator Laboratory: private communication.
13. SHEDLOVSKY, J.P.; HONDA, M.; REEDY, R.C.; EVANS, J.C., Jr.; LAL, D.; LINDSTROM, R.M.; DELANY, A.C.; ARNOLD, J.R.; LOOSLI, H.H.; FRUCHTER, J.S.; and FINKEL, R.C.: Pattern of Bombardment-Produced Radionuclides in Rock 10017 and in Lunar Soil. Proc. Apollo 11 Lunar Sci. Conf., Geomchim. Cosmochim. Acta, Suppl.I, Vol. 2, 1970, p. 1503.
14. FINKEL, R.C.; ARNOLD, J.A.; REEDY, R.C.; FRUCHTER, J.S.; LOOSLI, H.H.; EVANS, J.C.; SHEDLOVSKY, J.P.; and DELANY, A.C.: Depth Variation of Cosmogenic Nuclides in a Lunar Surface Rock. Paper presented at the Lunar Science Conference, Houston, Texas, January 11-14, 1971.
15. ARMSTRONG, T.W.; and ALSMILLER, R.G., Jr.: Calculation of Cosmogenic Radionuclides in the Moon and Comparison with Apollo Measurements. Oak Ridge National Laboratory Document ORNL-TM-3267 (in press.)

16. O'KELLEY, G.D.; ELDRIDGE, J.S.; SCHONFELD, E.; and BELL, P.R.: Comparative Radionuclide Concentrations and Ages of Apollo 11 and Apollo 12 Samples from Nondestructive Gamma-Ray Spectrometry. Paper presented at the Lunar Science Conference, Houston, Texas, January 11-14, 1971.

17. GABRIEL, T.A.; and SANTORO, R.T.: Calculation of the Long-Lived Activity in Soil Produced by 500-GeV Protons. Oak Ridge National Laboratory Document ORNL-TM-3262 (in press.)

18. ALSMILLER, R.G., Jr.; ARMSTRONG, T.W.; and COLEMAN, W.A.: Nucl. Sci. Eng., Vol. 42, 1970, p. 367

19. ALSMILLER, R.G., Jr.: Nucl. Sci. Eng., Vol. 27, 1967, p. 158.

20. HOLLY, F.; and TRAFTON, L.: Aerospace Med., Vol. 40, #12, 1969, p. 1441.